PHYSICAL REVIEW D **89,** 075008 (2014)

Search for MeV dark photons in a light-shining-through-walls experiment at CERN

S. N. Gninenko

Institute for Nuclear Research, Moscow 117312, Russia

(Received 5 September 2013; published 8 April 2014)

In addition to gravity, there might be another very weak interaction between the ordinary and dark matter transmitted by $U'(1)$ gauge bosons A' (dark photons) mixing with our photons. If such A''s exist, they could be searched for in a light-shining-through-a-wall experiment with a high-energy electron beam. The electron energy absorption in a calorimeter (CAL1) is accompanied by the emission of bremsstrahlung A''s in the reaction $eZ \to eZA'$ of electrons scattering on nuclei due to the $\gamma - A'$ mixing. A part of the primary beam energy is deposited in the CAL1, while the rest of the energy is transmitted by the A' through the "CAL1 wall" and deposited in another downstream calorimeter CAL2 by the e^+e^- pair from the $A' \to e^+e^-$ decay in flight. Thus, the A''s could be observed by looking for an excess of events with the two-shower signature generated by a single high-energy electron in the CAL1 and CAL2. A proposal to perform such an experiment to probe the still unexplored area of the mixing strength $10^{-5} \lesssim \epsilon \lesssim 10^{-3}$ and masses $M_{A'} \lesssim 100$ MeV by using 10–300 GeV electron beams from the CERN SPS is presented. The experiment can provide complementary coverage of the parameter space, which is intended to be probed by other searches. It has also a capability for a sensitive search for A''s decaying invisibly to dark-sector particles, such as dark matter, which could cover a significant part of the still allowed parameter space.

DOI: 10.1103/PhysRevD.89.075008 PACS numbers: 14.80.-j, 12.60.-i, 13.20.Cz, 13.35.Hb

I. INTRODUCTION

Understanding of the origin and properties of dark matter is a great challenge for particle physics and cosmology. Several models consider dark sectors of particles that, in addition to gravity, interact with ordinary matter by new, very weak forces transmitted by Abelian $U'(1)$ gauge bosons A' (dark or hidden photons for short), which could mix with our photons. In a class of these models, the A' can be massive and the $\gamma - A'$ mixing strength may be as large as $\epsilon \simeq 10^{-5}$–10^{-3}, which makes experimental searches for A''s interesting; for a recent review, see Refs. [1,2] and references therein.

The interaction between γ's and A''s is given by the kinetic mixing [1,3]

$$L_{\rm int} = -\frac{1}{2}\epsilon F_{\mu\nu}A'^{\mu\nu}, \tag{1}$$

where $F^{\mu\nu}$, $A'^{\mu\nu}$ are the ordinary and the dark photon fields, respectively, and parameter ϵ is their mixing strength. The kinetic mixing of Eq. (1) can be diagonalized, resulting in a nondiagonal mass term and $\gamma - A'$ mixing. Therefore, any source of photons could produce a kinematically permitted massive A' state according to the appropriate mixings. Then, depending on the A' mass, photons may oscillate into dark photons—similar to neutrino oscillations—or the A''s could decay, e.g., into e^+e^- pairs.

The aim of this work is to show that the still unexplored region of mixing strength $10^{-5} \lesssim \epsilon \lesssim 10^{-3}$ and A' masses $M_{A'} \lesssim 100$ MeV could be probed in a light-shining-through-a-wall-type experiment [1] with a high-energy electron beam. If such A''s exist, they would be short-lived particles which decay rapidly into e^+e^- pairs with a lifetime $< 10^{-10}$ s. We show that such decays could be observed by looking for events with the exotic signature—two isolated showers produced by a single electron in the detector. Compared to the beam-dump experiment searching for long-lived A''s, with the mixing typically $\epsilon \lesssim 10^{-4}$, the advantage of the proposed one is that for the parameter area $10^{-4} \lesssim \epsilon \lesssim 10^{-3}$ and $10 \lesssim M_{A'} \lesssim 100$ MeV, its sensitivity is roughly proportional to the mixing squared ϵ^2 associated with the A' production in the primary reaction and its subsequent fast decay at small distances $\lesssim$ a few m from the production vertex. While in the former case, it is proportional to ϵ^4, one ϵ^2 came from the A' production, and another ϵ^2 is from the probability of A' decays in a detector located at a large distance from the dump. The rest of the paper is organized in the following way. The experimental setup, method of search, background sources, and the expected sensitivity for the decay $A' \to e^+e^-$ are discussed in Sec. II. The search for the $A' \to$ invisible decay mode, background, and the expected sensitivity are discussed in Sec. III. Section IV contains concluding remarks.

II. THE EXPERIMENT TO SEARCH FOR $A' \to e^+e^-$ DECAYS

The process of the dark photon production and subsequent decay is a rare event. For the previously mentioned parameter space, it is expected to occur with the rate $\lesssim 10^{-13}$–10^{-9} with respect to the ordinary photon production rate. Hence, its observation presents a challenge for the

detector design and performance. The experimental setup specifically designed to search for the $A' \to e^+e^-$ decays is schematically shown in Fig. 1. The experiment could employ, e.g., the CERN SPS H4 e^- beam, which is produced in the target T2 of the CERN SPS and transported to the detector in an evacuated beam line tuned to a freely adjustable beam momentum from 10 up to 300 GeV/c [4]. The typical maximal beam intensity at ≃30–50 GeV is of the order of $5 \times 10^6 e^-$ for one typical SPS spill with 10^{12} protons on target. The typical SPS cycle for a fixed target (FT) operation lasts 14.8 s including 4.8 s spill duration. The maximal number of FT cycles is four per minute. The admixture of the other charged particles in the beam (beam purity) is below 10^{-2}, and the size of the beam at the calorimeter (CAL1) is of the order of a few cm^2.

The detector shown in Fig. 1 is equipped with a high density, compact electromagnetic (em) CAL1 to detect e^- primary interactions, high efficiency veto counters V1 and V2, two scintillating fiber counters (or proportional chambers) S1, S2, an electromagnetic calorimeter CAL2 located at the downstream end of the A' decay volume (DV) to detect e^+e^- pairs from $A' \to e^+e^-$ decays in flight, and a hadronic calorimeter (HCAL) used mainly for the $A' \to$ invisible decay mode (see Sec. V). For searches at low energies, the DV could be replaced by a Cherenkov counter to enhance the tagging of decay electrons.

The method of the search is the following. The A''s are produced through the mixing with bremsstrahlung photons from the electrons scattering off nuclei in the CAL1,

$$e^-Z \to e^-ZA'$$
$$A' \to e^+e^- \qquad (2)$$

as shown in Fig. 2. The reaction (2) typically occurs at the first few radiation lengths (X_0) of the detector. The bremsstrahlung A' then penetrates the rest of the CAL1

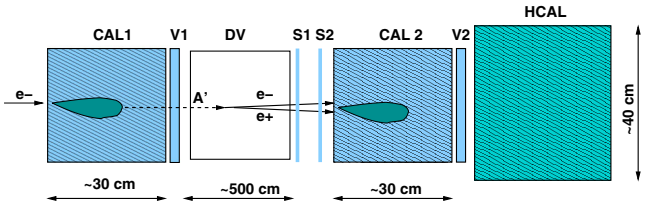

FIG. 1 (color online). Schematic illustration of the setup to search for dark photons in a light-shining-through-a-wall-type experiment at high energies. The incident electron energy absorption in the CAL1 is accompanied by the emission of bremsstrahlung A''s in the reaction $eZ \to eZA'$ of electrons scattering on nuclei due to the $\gamma - A'$ mixing, as shown in Fig. 2. The part of the primary beam energy is deposited in the CAL1, while the rest of the total energy is transmitted by the A' through the CAL1 wall. The A' penetrates the CAL1 and veto V1 without interactions and decays in flight in the DV into a narrow e^+e^- pair, which generates the second electromagnetic shower in the CAL2 resulting in the two-shower signature in the detector. The sum of energies deposited in the CAL1 + CAL2 is equal to the primary beam energy.

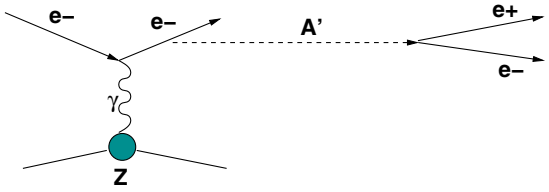

FIG. 2 (color online). Diagram illustrating the massive A' production in the reaction $e^-Z \to e^-ZA'$ of electrons scattering off a nuclei (A, Z) with the subsequent A' decay into an e^+e^- pair.

and the veto counter V1 without interactions and decays in flight into an e^+e^- pair in the DV. A fraction (f) of the primary beam energy $E_1 = fE_0$ is deposited in the CAL1. The CAL1's downstream part serves as a dump to absorb completely the em shower tail. For the radiation length $X_0 \lesssim 1$ cm and the total thickness of the CAL1 ≃30 cm, the energy leak from the CAL1 into the V1 is negligibly small. The remaining part of the primary electron energy $E_2 = (1-f)E_0$ is transmitted trough the "CAL1 wall" by the A' and deposited in the second downstream CAL2 via the A' decay in flight in the DV, as shown in Fig. 1. At high A' energies $E_{A'} \gtrsim 100$ GeV, the opening angle $\Theta_{e^+e^-} \simeq M_{A'}/E_{A'}$ of the decay e^+e^- pair is too small to be resolved in two separated tracks in the S1 and S2 or in two em showers in the CAL2, so the pairs are mostly detected as a single track or em shower.

The occurrence of $A' \to e^+e^-$ decays produced in e^-Z interactions would appear as an excess of events with two em-like showers in the detector, one shower in the CAL1 and another one in the CAL2, as shown in Fig. 1, above those expected from the background sources. The signal candidate events have the signature

$$S_{A'} = \mathrm{CAL1} \cdot \overline{V1} \cdot S1 \cdot S2 \cdot \mathrm{CAL2} \cdot \overline{V2} \cdot \overline{\mathrm{HCAL}} \qquad (3)$$

and should satisfy the following selection criteria:

(i) The starting point of (em) showers in the CAL1 and CAL2 should be localized within the few first X^0's.
(ii) The lateral and longitudinal shapes of both showers in the CAL1 and CAL2 are consistent with an electromagnetic one. The fraction of the total energy deposition in the CAL1 is $f \lesssim 0.1$, while in the CAL2 it is $(1-f) \gtrsim 0.9$ (see Fig. 2 and discussion below).
(iii) No energy deposition in the V1 and V2.
(iv) The signal (number of photoelectrons) in the decay counters S1 and S2 is consistent with the one expected from two minimum ionizing particle (mip) tracks. At low beam energies, $E_0 \lesssim 30$ GeV, two isolated hits in each counter are requested.
(v) The sum of energies deposited in the CAL1 + CAL2 is equal to the primary energy, $E_1 + E_2 = E_0$.

To estimate the sensitivity of the proposed experiment, a simplified feasibility study based on Geant4 [5] Monte Carlo simulations have been performed for 10 and 300 GeV

electrons. The CAL1 and CAL2 are the hodoscope arrays of the lead tungstate (PWO) heavy crystal counters ($X_0 \simeq 0.89$ cm), each of the size $10 \times 10 \times 300$ mm^3, allowing accurate measurements of the lateral and longitudinal shower shape. The veto counters are assumed to be 1–2 cm thick, high sensitivity LYSO crystal arrays with a high light yield of $\simeq 10^3$ photoelectrons per 1 MeV of deposited energy. It is also assumed that the veto's inefficiency for the mip detection is, conservatively, $\lesssim 10^{-4}$. Each of the decay counters S1 and S2 consists of two layers of scintillating fiber strips arranged, respectively, in the X and Y directions. Each strip consists of about 100 fibers of 1 mm square. The number of photoelectrons produced by a mip crossing the strip is $\simeq 20$. The energy resolution of the CAL1 and CAL2 as a function of the beam energy is taken to be $\frac{\sigma}{E} = \frac{2.8\%}{\sqrt{E}} \oplus 0.4\% \oplus \frac{142\ \mathrm{MeV}}{E}$ [6]. The energy threshold in the CAL1 is 0.5 GeV. The reported further analysis also takes into account passive materials from the DV tank walls.

The total number of A''s produced by n_e electrons impinging a target with thickness $t \gg X_0$ is [7]

$$n_{A'} \sim n_e C \frac{\epsilon^2 m_e^2}{M_{A'}^2}, \tag{4}$$

where parameter $C \simeq 10$ is only logarithmically dependent on the choice of target nucleus, and m_e is the electron mass; for recent works on heavy particles production through photon exchange with a nucleus, see, also, Refs. [8,9]. One can see that compared to the bremsstrahlung rate, the A' production rate is suppressed by a factor $\simeq \epsilon^2 m_e^2 / M_{A'}^2$. The A' energy spectrum is [7]

$$\frac{dn_{A'}}{dE_{A'}} \sim k \cdot x \left(1 + \frac{x^2}{3(1-x)}\right), \tag{5}$$

where k is a constant and $x = E_{A'}/E_0$. In Fig. 3, an example of the expected distributions of energy deposition in the CAL1 and CAL2 for selected events are shown for the initial e^- energy of 100 GeV. The spectra are calculated for the mixing strength $\epsilon = 3 \times 10^{-4}$ and corresponds to the case when the A' decay pass length $L_{A'}$ is in the range $L' < L_{A'} < L$, where L' is the length of the CAL1, and L is the distance between the A' production vertex and the CAL2. In this case, most of A''s decay outside of the CAL1 in the DV. One can see that the A' bremsstrahlung distribution is peaked at maximal beam energy.

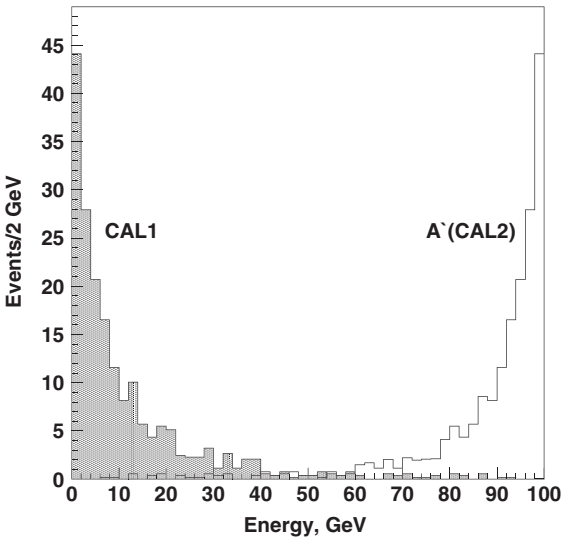

FIG. 3. Expected distributions of energy deposition for selected events (i) in the CAL1 (shaded) and (ii) in the CAL2 from the bremsstrahlung $A' \to e^+e^-$ decays in flight in the DV region. The spectra are calculated for the 10 MeV A''s produced by 100 GeV e^-'s in the CAL1 with momentum pointing towards the CAL2 fiducial area and the mixing strength $\epsilon = 3 \times 10^{-4}$. For this mixing value, most of the A''s decay outside of the CAL1 in the DV. The distributions are normalized to a common maximum.

A. Background

The background processes for the $A' \to e^+e^-$ decay signature $S_{A'}$ of Eq. (3) can be classified as being due to physical- and beam-related sources. To perform full detector simulation in order to investigate these backgrounds down to the level $\lesssim 10^{-12}$ would require a huge number of generated events resulting in a prohibitively large amount of computer time. Consequently, only the following identified as the most dangerous processes are considered and evaluated with reasonable statistics combined with numerical calculations:

(i) The leak of the primary electron energy into the CAL2 could be due to the bremsstrahlung process $e^-Z \to e^-Z\gamma$, when the emitted photon carries away almost all initial energy, while the final state electron with the much lower energy $E_{e^-} \simeq 0.1E_0$ is absorbed in the CAL1. The photon could punch through the CAL1 and V1 without interactions and produce an e^+e^- pair in the S1, which deposits all its energy in the CAL2. The photon could also be absorbed in a photonuclear reaction $\gamma W \to \pi^{\pm} X$ in the CAL1 resulting in, e.g., an energetic leading secondary pion or neutron accompanied by a small hadronic activity in the CAL1.
In the first case, to suppress this background, one has to use the CAL1 of enough thickness and as low a veto threshold as possible. Taking into account that the primary interaction vertex is selected to be within the few first X_0's and the probability for the bremsstrahlung photon to carry away $\gtrsim 90\%$ of the primary electron energy $\simeq 10^{-2}$ for the total remaining CAL1 + V1 thickness of $\simeq 30\ X_0$, the probability for the photon to punch through it without interaction per impinging electron is $\lesssim 10^{-12}$. Assuming that the photon conversion probability in S1 is 2×10^{-2}, this background is expected

to be at the negligible level $\lesssim 2\times 10^{-14}$. In the second case, the analysis results in a similar background level $\lesssim 10^{-13}$, mainly due to a small probability for secondary hadron to carry away almost all beam energy. Thus, the requirement to have low energy in the CAL1 and almost all beam energy deposited in the CAL2 is crucial for the background rejection of this type. If, for example, events are selected with the fraction of total energy deposited in the CAL1 $f \lesssim 0.3$, instead of $f \lesssim 0.1$, the signal-to-background ratio drops by a factor $\simeq 10$, while the signal efficiency is increased just by $\simeq 20\%$.

(ii) Punchthrough primary electrons, which penetrate the CAL1 and V1 without depositing much energy, could produce a fake signal event. It is found that this is also an extremely rare event.

The beam-related background can be categorized as being due to a beam particle misidentified as an electron. This background is caused by some pion, proton, and muon contamination in the electron beam.

(i) The first source of this type of background is due to the

$$p(\pi) + A \to n + \pi^0 + X, \qquad n \to \mathrm{CAL2} \tag{6}$$

reaction chain: (i) an incident proton (or a pion) produces a neutral pion with the energy $E_{\pi^0} \lesssim 0.1E_0$ and an energetic leading neutron carrying the rest of the primary collision with the nucleus (A, Z), (ii) the neutral pion decays into photons which generate an em shower in the CAL1, while (iii) the neutron penetrates the rest of the CAL1 and the V1 without interactions, scatters in the S1 producing low-energy secondaries, and deposits all its energy in the CAL2. The probability of such chain reactions to occur can be estimated as

$$P \simeq P_{p(\pi)} \cdot P_{\pi^0 n} \cdot P_{S1} \cdot P_n, \tag{7}$$

where $P_{p(\pi)}$, $P_{\pi^0 n}$, P_{S1}, P_n are, respectively, the level of the admixture of hadrons, $P_{p(\pi)} \lesssim 10^{-2}$, the probability for the incoming hadron to produce the $\pi^0 n$ pair in the CAL1, $P_{\pi^0 n} \simeq 10^{-4}$, the probability for the leading neutron to interact in S1, $P_{S1} \simeq 10^{-3}$, and the probability for the leading neutron to deposit all its energy in the CAL2, $P_n \simeq 10^{-3}$. This results in $P \lesssim 10^{-12}$. The probability for the neutron to interact in the S1 of thickness $\simeq 1$ mm or $\simeq 10^{-3}$ nuclear interaction length can be reduced significantly down to $P_{S1} \simeq 10^{-4}$ by replacing it, e.g., with a thin wire chamber counter. This leads to $P \lesssim 10^{-13}$. At low energies $E_0 \lesssim 30$ GeV, the requirement to have two hits in the S1 would significantly suppress the background further.

Note that the total cross section for the reaction $p(\pi) + A \to \pi^0 + n + X$ with the leading neutron in the final state has not yet been studied in detail for the wide class of nuclei and full range of hadron energies. To perform an estimate of the $P_{\pi^0 n}$ value, we use available data from the ISR experiment at CERN, which measured leading neutron production in pp collisions at $\sqrt{s}$ in the range of 20 to 60 GeV [10,11]. For these energies, the invariant cross sections measured as a function of x_F (Feynman x) and p_T were found to be in the range $0.1 \lesssim E\frac{d^3\sigma}{d^3p} \lesssim 10$ mb/GeV^2 for $0.9 \lesssim x_F \lesssim 1$ and $0 \lesssim p_T \lesssim 0.6$ GeV [10]. Taking this into account, the cross sections for leading neutron production in our energy range are evaluated by using the Bourquin-Gaillard formula, which gives the parametric form of the invariant cross section for the production in high-energy hadronic collisions of many different hadrons over the full phase space, for more details, see, e.g., Ref. [12]. The total leading neutron production cross sections in $p(\pi)A$ collisions are calculated from its linear extrapolation to the target atomic number.

In another scenario, the leading neutron could interact in the very last downstream part of the veto counter producing leading π^0 without being detected. The neutral pion decays subsequently into 2γ or $e^+e^-\gamma$. The background from this event's chain is also found to be very small.

(ii) The fake signature $S_{A'}$ arises when the incoming pion produces a low-energy neutral pion in the very beginning of the CAL1, escapes detection in the V1 due to its inefficiency, and either deposits all its energy in the CAL2 or decays in flight in the DV into an $e\nu$ pair with the subsequent electron energy deposition in the CAL2. In the first case, also relevant to protons, considerations similar to the previous one show that this background is expected to be at the level $\lesssim 10^{-13}$. In the second case, taking into account the probability for the $\pi \to e\nu$ decay in flight and the fact that the decay electron would typically have about one half of the pion energy results in suppression of this background to the level $< 10^{-15}$.

(iii) Another type of background is caused by the muon contamination in the beam. The muon could produce a low-energy photon in the CAL1, which would be absorbed in the detector, then penetrates the V1 without being detected, and after producing signals in the S1 and S2 deposits all its energy in the CAL2 through the emission of a hard bremsstrahlung photon:

$$\mu + Z \to \gamma + \mu + Z, \qquad \mu \to \mathrm{CAL2}. \tag{8}$$

The probability for the events chain (8) is estimated to be $P \lesssim 10^{-14}$. Similar to Eq. (6), this estimate is obtained assuming that the muon contamination in the beam is $\lesssim 10^{-2}$, the probability for the muon to cross the V1 without being detected is $\lesssim 10^{-4}$, and the probability for the μ to deposit all its energy in the

CAL2 is $\lesssim 10^{-7}$. Here, it is also taking into account that the muon should stop in the CAL2 completely to avoid being detected in the veto V2. The additional suppression factor is due to the requirement to have two mip-like signals in the decay counters.

(iv) One more background can be due the event chain

$$\mu + Z \to \mu + \gamma + Z, \qquad \mu \to e\nu\nu, \tag{9}$$

when the incident muon produces in the initial CAL1 part a low-energy bremsstrahlung photon, escapes detection in the V1, and then decays in flight in the DV into $e\nu\nu$. There are several suppression factors for this source of background: (i) the relatively long muon lifetime resulting in a small probability to decay, and (ii) the presence of two neutrinos in the μ decay. The decay electron energy deposition in the CAL2 is typically significantly smaller than the primary energy E_0 and (iii) the requirement to have double mip energy deposition in the beam counters S1 and S2. All these factors lead to the expectation for this background to be at the level at least $\lesssim 10^{-14}$.

(v) A random superposition of uncorrelated events occurring during the detector gate time could also result in a fake signal. However, taking into account the selection criteria of signal events and the fact that the beam time intensity profile is flat during the spill duration results in a small number of these background events $\lesssim 10^{-14}$.

In Table I, contributions from the all background processes are summarized. The total background is conservatively at the level $\lesssim 3 \times 10^{-13}$ and is dominated by the admixture of hadrons in the electron beam. This means that the search accumulated up to $\simeq 10^{13}$ e^- events is expected to be background free. To evaluate background in the signal region, one could perform independent direct measurements of its level with the same setup by using pion and muon beams of proper energies.

B. Expected sensitivity

The significance of the $A' \to e^+e^-$ decay discovery with such a detector scales as [13,14]

$$S = 2 \cdot (\sqrt{n_{A'} + n_b} - \sqrt{n_b}), \tag{10}$$

TABLE I. Expected contributions to the total level of background from different background sources (see text for details).

Source of background	Expected level
Punchthrough e^-'s or γ's	$\lesssim 10^{-13}$
Hadronic reactions	$\lesssim 2 \times 10^{-13}$
μ reactions	$\lesssim 10^{-14}$
Accidentals	$\lesssim 10^{-14}$
Total (conservative)	$\lesssim 3 \times 10^{-13}$

where $n_{A'}$ is the number of observed signal events (or the upper limit of the observed number of events), and n_b is the number of background events.

For a given number of e^-'s on the target (CAL1) of length L', $n_e t$ (here, n_e is the electron beam intensity and t is the experiment running time) and A' flux $dn_{A'}/dE_{A'}$, the expected number of $A' \to e^+e^-$ decays occurring within the fiducial volume of the DV with the subsequent energy deposition in the CAL2 located at a distance L from the A' production vertex is given by

$$n_{A'} \sim n_e t \int A \frac{dn_{A'}}{dE_{A'}} \exp\left(-\frac{L' M_{A'}}{p_{A'} \tau'_A}\right) \times \left[1 - \exp\left(-\frac{L M_{A'}}{p_{A'} \tau'_A}\right)\right] \frac{\Gamma_{e^+e^-}}{\Gamma_{\rm tot}} \varepsilon_{e^+e^-} dE_{A'} dV, \tag{11}$$

where $p_{A'}$ is the A' momentum, $\tau_{A'}$ is its lifetime at the rest frame, $\Gamma_{e^+e^-}$, $\Gamma_{\rm tot}$ are the partial and total A'-decay widths, respectively, and $\varepsilon_{e^+e^-} (\simeq 0.9)$ is the e^+e^- pair reconstruction efficiency. The flux of A''s produced in reaction (2) is calculated by using the A' production cross section in the e^-Z collisions from Ref. [7] (an example of the flux calculation is shown in Fig. 3). The acceptance A of the CAL2 detector is calculated tracing A''s produced in the CAL1 to the CAL2. The corresponding $A' \to e^+e^-$ decay rate is given by

$$\Gamma(A' \to e^+e^-) = \frac{\alpha}{3} \epsilon^2 M_{A'} \sqrt{1 - \frac{4m_e^2}{M_{A'}^2}} \left(1 + \frac{2m_e^2}{M_{A'}^2}\right). \tag{12}$$

It is assumed that this decay mode is dominant and the branching ratio $\frac{\Gamma(A' \to e^+e^-)}{\Gamma_{\rm tot}} \simeq 1$.

If no excess events are found, the obtained results can be used to impose bounds on the $\gamma - A'$ mixing strength as a function of the dark photon mass. Taking Eqs. (10)–(12) into account and using the relation $n_{A'}(M_{A'}) < n_{A'}^{90\%}(M_{A'})$, where $n_{A'}^{90\%}(M_{A'})$ is the 90% C.L. upper limit for the number of signal events from the decays of the A' with a given mass $M_{A'}$, one can determine the expected 90% C.L. exclusion area in the $(M_{A'}; \epsilon)$ plane from the results of the experiment. For the background-free case $[n_{A'}^{90\%}(M_{A'}) = 2.3$ events], the exclusion regions corresponding to accumulated statistics 10^9 e^-'s at 300 GeV (H4-a), 10^{11} e^-'s at 300 GeV (H4-b), and 10^{13} e^-'s at 10 GeV (H4-c) are shown in Fig. 4. One can see that these exclusion areas are complementary to the ones expected from the planned APEX (full run) and DarkLight experiments, which are also shown for comparison [2]. For a review of all experiments, which intend to probe a similar parameter space, see Ref. [2] and references therein. Shown also are areas excluded from the electron (g-2) considerations (a_e) [15], by the results of the electron beam-dump experiments E141 [16] and E774 [17], by searches at LAL Orsay [18], U70 (Protvino) [19], and KLOE [20], from

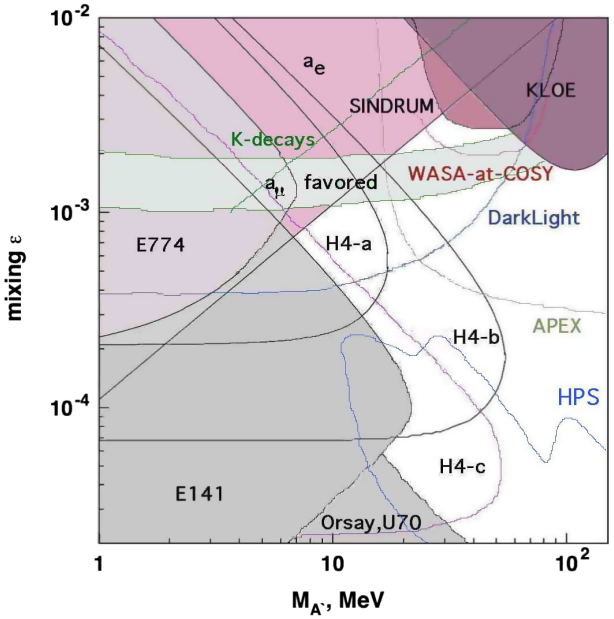

FIG. 4 (color online). Exclusion region in the $(M_{A'}; \epsilon)$ plane obtained in the present work from the expected results of the experiments accumulated 10^9 e^-'s at 300 GeV (H4-a), 10^{11} e^-'s at 300 GeV (H4-b), and 10^{13} e^-'s at 10 GeV (H4-c). Shown are also areas excluded from the electron (g-2) considerations (a_e) [15], by the results of the electron beam-dump experiments E141 [16] and E774 [17], by searches at LAL Orsay [18], U70 (Protvino) [19], and KLOE [20], from kaon decays [21] and data of the experiment SINDRUM [22,23], and by the WASA-at-COSY Collaboration [24]. Expected sensitivities of the planned APEX (full run), HPS, and DarkLight experiments are also shown for comparison [2]. For a review of all experiments, which intend to probe a similar parameter space, see Ref. [2] and references therein. In addition, the light grey area shows the $\pm 2\sigma$ preferred band from the muon g-2 anomaly consideration.

kaon decays [21] and data of the experiment SINDRUM [22,23], and by the WASA-at-COSY Collaboration [24]. For cosmological constraints on dark-matter particles charged under a hidden gauge group, see, e.g., Ref. [25].

The statistical limit on the sensitivity of the proposed experiment is set mostly by the value of the mixing strength. Thus, to accumulate a large number of events is important. As one can see from Eq. (11), the obtained exclusion regions are also sensitive to the choice of the length L' of the CAL1, which should be as short as possible. Assuming the average H4 beam rate $n_e \gtrsim 10^5 e^-/\mathrm{s}$ at $E_0 \simeq 200$–300 GeV, we anticipate $\simeq 3 \times 10^{11}$ e^-'s on CAL1 during $\simeq 1$ month of running time for the experiment. At lower energies, the e^- beam intensity is increased and much higher statistics can be accumulated. Note, however, that since the decay time of the PWO/LYSO light signal is $\tau \lesssim 50$ ns, the maximally allowed electron counting rate has to be $\lesssim 1/\tau \simeq 10^7 e^-/\mathrm{s}$ to avoid a significant pile-up effect. To minimize dead time, one could use first-level trigger rejecting events with the CAL2 energy deposition less than, say, the energy $\simeq 0.9 E_0$ and, hence, run the experiment at a higher rate.

In the case of the signal observation, to cross-check the result, one could remove DV and put the CAL2 behind the CAL1. This would not affect the main background sources and still allow the A''s production but with their decays in front of the CAL2 being suppressed. In this case, the distribution of the energy deposition in the CAL1 and CAl2 would contain mainly background events, while the signal from the decays $A' \to e^+e^-$ should be reduced. The background can also be independently studied with a high-energy muon and pion beams. The evaluation of the A' mass could be obtained from the results of measurements at different distances L and beam energies. Finally note that the performed analysis gives an illustrative order of magnitude for the sensitivity of the proposed experiment and may be strengthened by more accurate and detailed simulations of the H4 beam line and experimental setup.

III. THE EXPERIMENT TO SEARCH FOR THE DECAY $A' \to$ invisible

The A''s could also decay invisibly into a pair of dark-matter particles $\chi\bar{\chi}$, see Refs. [26,27] and references therein. The process of the dark photon production and subsequent invisible decay

$$e^-Z \to e^-ZA'$$
$$A' \to \text{invisible} \tag{13}$$

shown in Fig. 5 is expected to be a very rare event. For the previously mentioned parameter space, it is expected to occur with the rate $\lesssim 10^{-10}$ with respect to the ordinary photon production rate. Hence, its observation presents a challenge for the detector design and performance.

A. The setup

The detector specifically designed to search for the $A' \to$ invisible decays is schematically shown in Fig. 1. The experiment employs the same very clean high-energy e^- beam for the search for the $A' \to e^+e^-$ decays. The detector shown in Fig. 1 is additionally equipped with a massive HCAL located at the downstream end of the setup to detect all final state products from the primary reaction $e^-Z \to$ anything (see below).

The method of the search is the following. The A''s are produced through the mixing with bremsstrahlung photons

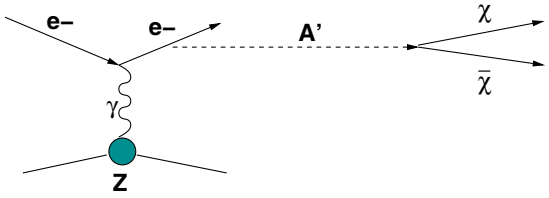

FIG. 5 (color online). Diagram illustrating the massive A' production in the reaction $e^-Z \to e^-ZA'$ of electrons scattering off a nuclei (A, Z) with the subsequent A' decay into a $\chi\bar{\chi}$ pair.

from the electrons scattering off nuclei in the CAL1. The reaction (13) typically occurs in the first few radiation lengths of the detector. The bremsstrahlung A' then penetrates the rest of the setup without interactions and decays in flight invisibly, $A' \to$ invisible, into a pair of dark-matter particles, which also penetrate the rest of the setup without interaction. Similar to the previous case, the fraction f of the primary beam energy $E_1 = fE_0$ is deposited in the CAL1 by the scattered electron. The CAL1's downstream part serves as a dump to absorb completely the em shower tail. For the total thickness of the CAL1 $\simeq 30X_0$, the energy leak from the CAL1 into the V1 is negligibly small. The remaining part of the primary electron energy $E_2 = (1-f)E_0$ is carried away by the products of the decay $A' \to \chi\bar{\chi}$. In order to suppress background due to the detection inefficiency, the detector must be longitudinally completely hermetic. To enhance detector hermeticity, the hadronic calorimeter with a total thickness $\simeq 20\lambda_{\rm int}$ (nuclear interaction lengths) is placed behind the CAL2, as shown in Fig. 1. Under the assumption that the A' decays dominantly into the invisible final state, the CAL1 is not constrained in length anymore, as it was for the case of $A' \to e^+e^-$ decays. The CAL1 (and CAL2) could be, e.g., a hodoscope array of the PWO crystal counters or another em calorimeter of similar performance. The occurrence of $A' \to$ invisible decays produced in e^-Z interactions would appear as an excess of events with a single em shower in the CAL1, see Fig. 1, and zero energy deposition in the rest of the detector, above those expected from the background sources. The signal candidate events have the signature

$$S_{A'} = \mathrm{CAL1} \cdot \overline{\mathrm{V1} \cdot \mathrm{S1} \cdot \mathrm{S2} \cdot \mathrm{CAL2} \cdot \mathrm{V2} \cdot \mathrm{HCAL}}, \quad (14)$$

and should satisfy the following selection criteria:

(i) The starting point of (em) showers in the CAL1 should be localized within the few first X_0's.

(ii) The lateral and longitudinal shapes of the shower in the CAL1 are consistent with an electromagnetic one. The fraction of the total energy deposition in the CAL1 is $f \lesssim 0.1$, while in the CAL2, it is zero.

(iii) No energy deposition in the V1, S1, S2, CAL2, V2, and HCAL.

B. Background

The background reactions resulting in the signature of Eq.refsigninv can be classified as being due to physical- and beam-related sources. Similar to the case of the decay $A' \to e^+e^-$, to perform a full detector simulation in order to investigate these backgrounds down to the level $\lesssim 10^{-10}$ would require a prohibitively large amount of computer time. Consequently, only the following background sources identified as the most dangerous are considered and evaluated with reasonable statistics combined with numerical calculations:

(i) One of the main background sources is related to the low-energy tail in the energy distribution of beam electrons. This tail is caused by the electron interactions with a passive material, such as entrance windows of the beam lines, residual gas, etc. Another source of low-energy electrons is due to the pion or muon decays in flight in the beam line. The uncertainties arising from the lack of knowledge of the dead material composition in the beam line are potentially the largest source of systematic uncertainty in accurate calculations of the fraction and energy distribution of these events. An estimation shows that the fraction of events with energy below $\lesssim 10$ GeV in the electron beam tuned to 100 GeV could be as large as 10^{-8}. Hence, the sensitivity of the experiment could be determined by the presence of such electrons in the beam, unless one takes special measures to suppress this background.
To improve the high-energy electrons selection and suppress background from the possible admixture of low-energy electrons, one can use a tagging system utilizing the synchrotron radiation (SR) from high-energy electrons in a dipole magnet installed upstream of the detector, as schematically shown in Fig. 6. The basic idea is that, since the critical SR photon energy is $(\hbar\omega)^c_\gamma \propto E_0^3$, the low-energy electrons in the beam could be rejected by using the cut, e.g., $E_\gamma > 0.3(\hbar\omega)^c_\gamma$, on the energy deposited in an x-ray detector shown in Fig. 6. For detection of the SR photons in vacuum, one can utilize the inorganic LYSO crystal with a high light yield. The possibility of identifying electrons by detecting their synchrotron radiation has been demonstrated previously, see, e.g., Ref. [28]. Note that additionally, electrons with energy $\lesssim 10$ GeV will be deflected by the magnet at an angle which is larger than those for

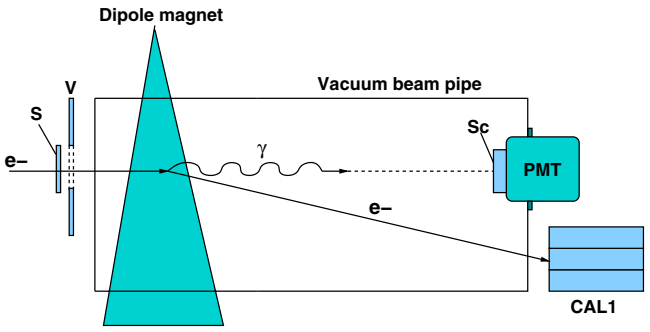

FIG. 6 (color online). The scheme of the additional tagging of high-energy electrons in the beam by using the electron synchrotron radiation in the banding magnetic dipole. The synchrotron radiation photons are detected by a γ detector by using the LYSO inorganic crystal (Sc) capable for the work in vacuum. The crystal is viewed by a high quantum efficiency photodetector, e.g., PMT, SiPM, or APD. The beam defining counters S and veto V are also shown.

100 GeV e^-, and, hence do not hit the CAL1. However, low-energy electrons could appear in the beam after the magnet due to the muon $\mu \to e\nu\nu$ or pion $\pi \to e\nu$ decays in flight. Since μs and πs do not emit SR photons with energy above the cut, this source of background will also be suppressed.

(ii) The fake signature of Eq. (14) could also arise when either (i) a beam hadron produces a low-energy neutral pion in the very beginning of the CAL1 and then escapes detection in the rest of the detector, or (ii) a leading hadron h from the reaction $eA \to ehX$ occurring in a very upstream part of the CAL1 is not detected. In the first case, the background is suppressed by the requirement of the presence of the synchrotron photon in the beam line. In the second case, background is dominated by the incomplete hermeticity of the detector. The leak of energy could be due to the production of a leading neutral hadron, such as a neutron and/or K_L^0, which punch through the CAL2 and HCAL without depositing energy above a certain threshold $E_{\rm th}$. An event with the sum of energy released in the CAL2 and HCAL below $E_{\rm th}$ is considered a "zero-energy" event. The punch-through probability is defined by $\exp(-L_{\rm tot}/\lambda_{\rm int})$, where $L_{\rm tot}$ is the (CAL2 + HCAL) sum length. It is of the order 10^{-9} for the total thickness of the CAL2 and HCAL about 21 $\lambda_{\rm int}$. This value should be multiplied by a conservative factor $\lesssim 10^{-4}$, which is the probability of single leading hadron photo- or electroproduction in the CAL1. Taking this into account results in the final estimate of $\lesssim 10^{-13}$ for the level of this background per incoming electron.

(iii) The HCAL nonhermeticity for high-energy hadrons was cross-checked with Geant4-based simulations. The low-energy tail in the distribution of energy deposited by $\simeq 10^7$ simulated 100 GeV neutrons in the CAL2 + HCAL was fitted by a smooth polynomial function and extrapolated to the lowest energy region in order to evaluate the number of events below a certain threshold $E_{\rm th}$. This procedure resulted in an estimate of the (CAL2 + HCAL)-nonhermeticity defined as the ratio of the number of events below the threshold $E_{\rm th}$ to the total number of incoming particles: $\eta = n(E < E_{\rm th})/n_{\rm tot}$. For the energy threshold $E_{\rm th} \simeq 1$ GeV the nonhermeticity is expected to be at the level $\eta \lesssim 10^{-9}$. Taking into account the probability to produce the single leading hadron per incoming electron to be $P_h \lesssim 10^{-4}$ results in an overall level of this background of $\lesssim 10^{-13}$, in agreement with the previous rough estimate.

In Table II, contributions from the all background processes are summarized for the beam energy of 100 GeV. The total background is conservatively at the level $\lesssim 10^{-12}$. This means that the search that accumulated up to $\simeq 10^{12}$ e^- events is expected to be background free.

TABLE II. Expected contributions to the total level of background from different background sources estimated for the beam energy 100 GeV (see text for details).

Source of background	Expected level
Punchthrough e^-'s or γ's	$\lesssim 10^{-13}$
HCAL nonhermeticity	$\lesssim 10^{-13}$
e^- low-energy tail, $E_e \lesssim 0.1E_0$	$\lesssim 10^{-13}$
μ reactions	$\lesssim 10^{-13}$
e^--induced photo-nuclear reactions	$\lesssim 10^{-13}$
Total (conservative)	$\lesssim 5 \times 10^{-13}$

C. Expected sensitivity

Using considerations which are similar to those of Sec. II B, the expected exclusion areas in the plane $(\epsilon, M_{A'})$ derived for the background-free case are shown in Fig. 7 for accumulated statistics of 10^9 (light blue) and 10^{12} (blue) e^-'s with energy 100 GeV. The only assumption used is that the A''s decay dominantly to the invisible final state $\chi\bar{\chi}$ if the A' mass $M_{A'} > 2m_\chi$, for more details, see Ref. [29]. Similar to the case of the visible A' decay search, the statistical limit on the sensitivity of the proposed experiment is proportional to ϵ^2 and is mostly set by its value. Thus, it is important to accumulate a large number of events. In the case of the $A' \to$ invisible signal observation, several methods could be used to cross-check the result. For instance, to test whether the signal is due to the HCAL nonhermeticity or not, one could perform several measurements with different HCAL thicknesses. In this case, the expected background level can be obtained by extrapolating the results to a very large (infinite) HCAL thickness.

IV. CONCLUSION

Due to their specific properties, dark photons are an interesting probe of physics beyond the standard model both from the theoretical and experimental viewpoints. We proposed to perform a light-shining-through-a-wall experiment dedicated to the sensitive search for dark photons in the still unexplored area of the mixing strength $10^{-5} \lesssim \epsilon \lesssim 10^{-3}$ and masses $M_{A'} \lesssim 100$ MeV by using available 10–300 GeV electron beams from the CERN SPS. If A''s exist, their dielectron decays $A' \to e^+e^-$ could be observed by looking for events with the two-shower topology of energy deposition in the detector. The key point for the experiment is an observation of events with almost all beam energy deposition in the CAL2 located behind the CAL1 wall. The advantage of the proposed search is that for the area of the mixing $10^{-4} \lesssim \epsilon \lesssim 10^{-3}$ and masses $10 \lesssim M_{A'} \lesssim 100$ MeV, its sensitivity is roughly proportional to the mixing squared, ϵ^2, different from the case of a search for a long-lived A', where the number of signal events is $\propto \epsilon^4$.

A feasibility study of the experimental setup showed that the sensitivity of the search for the $A' \to e^+e^-$ decay in ratio of cross sections $\frac{\sigma(e^-Z \to e^-ZA')}{\sigma(e^-Z \to e^-Z\gamma)}$ at the level of $\lesssim 10^{-13}$

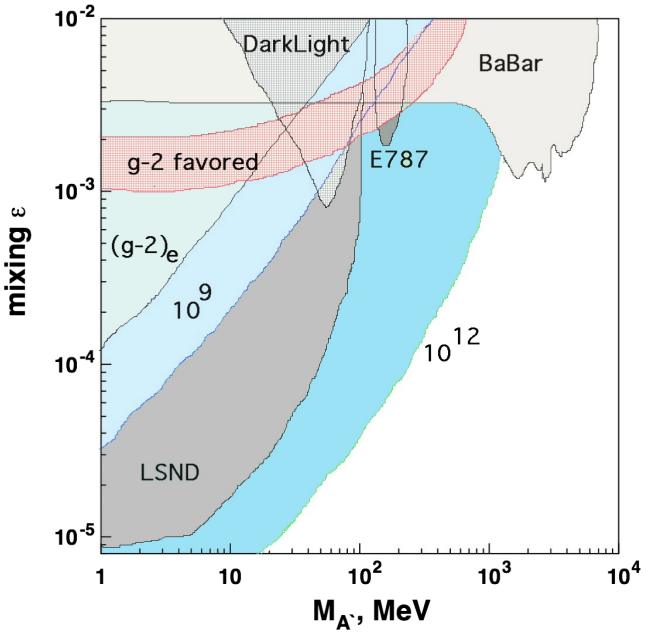

FIG. 7 (color online). Constraints in the ϵ vs $M_{A'}$ plane for invisibly decaying A' into a pair of light dark-matter particles $\chi\bar{\chi}$ provided $M_{A'} > 2m_{\chi}$. The light blue and blue areas show the expected 90% C.L. exclusion areas corresponding, respectively, to 10^9 and 10^{12} accumulated electrons at 100 GeV for the background-free case. Other existing constraints, mostly adapted from Ref. [27], are also shown. The constraint from the *BABAR* monophoton search is given as the light grey shaded region. Further limits are shown from the anomalous magnetic moment of the electron $[(g-2)_e]$, and DarkLight, the rare kaon decay $K^+ \to \pi^+ A'$ (E787), and LSND experiments. The LSND area is determined assuming $A' - \chi$ coupling $\alpha_D = 0.1$, and that χ cannot decay to other light dark-sector states which do not interact with A''s [30]. The red shaded region is preferred in order to explain the discrepancy between the measured and the predicted value of the anomalous magnetic moment of the muon. A more complete plot including various other constraints from performed and planned experiments can be found in Ref. [29].

could be achieved. This sensitivity could be obtained with a setup optimized for several of its properties. Namely, (i) the intensity and purity of the primary electron beam, (ii) the high efficiency of the veto counters, (iii) the high number of photoelectrons from decay counters S1 and S2, and (iv) the good energy, time resolution, and capability to measure accurately the longitudinal and lateral shape of showers in both CAL1 and CAL2 are of importance. A large amount of high-energy electrons and high background suppression is crucial to improve the sensitivity of the search. To obtain the best sensitivity for a particular parameter region, the choice of the energy and intensity of the beam as well as the background level should be compromised. In the case of nonobservation, the expected exclusion areas are complementary to the ones from the planned APEX (full run), DarkLight, and other experiments intended to probe a similar parameter space [2].

The experiment has also the capability for a sensitive search for A''s decaying invisibly to dark-sector particles, such as dark matter. Our feasibility study showed that a sensitivity for the search of the $A' \to$ invisible decay mode in branching fraction $\mathrm{Br}(A') = \frac{\sigma(e^- Z \to e^- Z A'), A' \to \mathrm{invisible}}{\sigma(e^- Z \to e^- Z \gamma)}$ at the level below a few parts in 10^{13} is in reach. The intrinsic background due to the presence of low-energy electrons in the beam can be suppressed by using a tagging system, which is based on the detection of synchrotron radiation of high-energy electrons. The search would allow us to cover a significant fraction of the yet unexplored parameter space for the $A' \to$ invisible decay mode.

This proposal provided interesting motivations for the search for light dark-matter particles in order to perform it at CERN in the near future. The experiment might be a sensitive probe of new physics that is complementary to collider experiments. The required high-energy, intensity, and purity electron beams could also be available at future facilities such as the CLIC [31].

ACKNOWLEDGMENTS

I would like to thank S. Andreas, P. Crivelli, S. Donskov, D. Gorbunov, M. Kirsanov, N. Krasnikov, L. Di Lella, V. Matveev, V. Polyakov, A. Radionov, A. Ringwald, A. Rubbia, V. Samoylenko, and K. Zioutas for useful discussions and comments and A. Fabich and L. Gatignon for valuable comments on the CERN SPS beam lines.

[1] J. Jaeckel and A. Ringwald, Annu. Rev. Nucl. Part. Sci. **60**, 405 (2010).
[2] J. L. Hewett *et al.*, arXiv:1205.2671.
[3] L. B. Okun, Zh. Eksp. Teor. Fiz. **83**, 892 (1982) [Sov. Phys. JETP **56**, 502 (1982)].
[4] See, for example, http://sba.web.cern.ch/sba/.
[5] S. Agostinelli *et al.* (Geant4 Collaboration), Nucl. Instrum. Methods Phys. Res., Sect. A **506**, 250 (2003); J. Allison *et al.* (Geant4 Collaboration), IEEE Trans. Nucl. Sci. **53**, 270 (2006).
[6] P. Adzic *et al.* (CMS Collaboration), JINST **5**, P03010 (2010).
[7] J. D. Bjorken, R. Essig, P. Schuster, and N. Toro, Phys. Rev. D **80**, 075018 (2009).
[8] M. Masip, P. Masjuan, and D. Meloni, J. High Energy Phys. 01 (2013) 106.

[9] A. Radionov, Phys. Rev. D **88**, 015016 (2013).
[10] W. Flauger and F. Mönnig, Nucl. Phys. **B109**, 347 (1976).
[11] J. Engler *et al.*, Nucl. Phys. **B84**, 70 (1975).
[12] S. N. Gninenko, Phys. Lett. B **713**, 244 (2012).
[13] S. I. Bityukov and N. V. Krasnikov, Mod. Phys. Lett. A **13**, 3235 (1998).
[14] S. I. Bityukov and N. V. Krasnikov, Nucl. Instrum. Methods Phys. Res., Sect. A **534**, 152 (2004).
[15] M. Endo, K. Hamaguchi, and G. Mishima, Phys. Rev. D **86**, 095029 (2012).
[16] E. M. Riordan *et al.*, Phys. Rev. Lett. **59**, 755 (1987).
[17] A. Bross, M. Crisler, S. H. Pordes, J. Volk, S. Errede, and J. Wrbanek, Phys. Rev. Lett. **67**, 2942 (1991).
[18] S. Andreas, C. Niebuhr, and A. Ringwald, Phys. Rev. D **86**, 095019 (2012).
[19] J. Blümlein and J. Brunner, Phys. Lett. B **701**, 155 (2011).
[20] F. Archilli *et al.*, Phys. Lett. B **706**, 251 (2012).
[21] T. Beranek and M. Vanderhaeghen, Phys. Rev. D **87**, 015024 (2013).
[22] S. N. Gninenko, Phys. Rev. D **87**, 035030 (2013).
[23] R. Meijer Drees *et al.* (SINDRUM Collaboration), Phys. Rev. Lett. **68**, 3845 (1992).
[24] P. Adlarson *et al.* (WASA-at-COSY Collaboration), Phys. Lett. B **726**, 187 (2013).
[25] D.-C. Dai, K. Freese, and D. Stojkovic, J. Cosmol. Astropart. Phys. 06 (2009) 023.
[26] R. Essig, J. A. Jaros, W. Wester, P. H. Adrian, S. Andreas, T. Averett, O. Baker, B. Batell *et al.*, arXiv:1311.0029.
[27] R. Essig, J. Mardon, M. Papucci, T. Volansky, and Y.-M. Zhong, J. High Energy Phys. 11 (2013) 167.
[28] J. S. Dworkin, P. T. Cox, E. C. Dukes, O. E. Overseth, R. Handler, R. Grobel, A. Jaske, B. Lundberg *et al.*, Nucl. Instrum. Methods Phys. Res., Sect. A **247**, 412 (1986).
[29] S. Andreas *et al.*, arXiv:1312.3309.
[30] P. deNiverville, M. Pospelov, and A. Ritz, Phys. Rev. D **84**, 075020 (2011).
[31] H. Abramowicz *et al.* (CLIC Detector and Physics Study Collaboration), arXiv:1307.5288.